Effect of Grain Refinement on Structure Evolution, "Floating" Grains, and Centerline Macrosegregation in Direct-Chill Cast AA2024 Alloy Billets

R. NADELLA, D.G. ESKIN, and L. KATGERMAN

Direct-chill (DC) cast billets 192 mm in diameter of an Al-Cu-Mg alloy were examined in detail with the aim to reveal the effects of grain refining (GR) and casting speed on structure, "floating" grains, and centerline macrosegregation. Experimental results show that grain size and dendrite arm spacing (DAS) tend to coarsen toward the billet center with a local refinement DAS in the center. In GR billets, grain size does not change much with the cooling rate, casting speed, and grain refiner amount. Coarse-DAS (floating) grains are observed around the billet axis regardless of GR and the amount of Ti, though their amount is significantly higher in GR billets. Macrosegregation profiles show a negligible influence of GR, while the effect of casting speed is large. The concept of solute-depleted floating grains contributing to the centerline macrosegregation is substantiated by microsegregation measurements, which show that, independent of GR, coarse dendrite branches have a depleted concentration plateau in contrast to the fine dendrite arms.

DOI: 10.1007/s11661-007-9423-z

I. INTRODUCTION

DIRECT-CHILL (DC) casting is a major route to producing large aluminum ingots, which are used for downstream processing. During casting, grain refining (GR) is normally employed to achieve finer equiaxed grains. The fine-grained structure decreases the sensitivity to hot cracking during casting and improves the mechanical properties of the as-cast metal. However, the relation between structure refinement and the occurrence of defects such as hot cracking, macrosegregation, *etc*. is still not fully understood. Macrosegregation, which is the nonhomogeneous distribution of alloying elements over a large length scale, needs to be minimized as it affects the quality of the finished product and limits the size and the allowable speed at which the DC cast billets are produced. Unlike microsegregation, which is normally minimized or eliminated during homogenization, macrosegregation remains essentially unaffected by heat treatments. This leaves us with little choice but to control it during the casting stage. The fundamental reasons for the macrosegregation is the partitioning of alloying elements between the solid and liquid phases during solidification and the relative movement of the solid and liquid phases in the two-phase region of a casting.

R. NADELLA, Postdoctoral Researcher, and D.G. ESKIN, Senior Scientist, are with the Netherlands Institute for Metals Research, 2628CD, Delft, The Netherlands. Contact e-mail: d.g.eskin@tudelft.nl L. KATGERMAN, Professor, is with the Department of Materials Science and Engineering, Delft University of Technology, 2628CD, Delft, The Netherlands.

Manuscript submitted August 27, 2007.
Article published online December 13, 2007

During DC casting, the process parameters (*e.g*., casting speed, melt temperature, and water flow rate) influence the cooling conditions and shape of the two-phase (liquid-solid) region, which determines to a large extent the structure and associated defect formation.[1,2] This region can be conventionally divided into "slurry" zone and "mushy" zone, based on the definition of coherency temperature,[3] at which solid grains start to interact with each other. The part of the two-phase region above the coherency isotherm can be called a slurry, as the liquid and solid phases there can freely move relative to each other. Below the coherency isotherm, the solid phase cannot move on the macroscale, and this region can be called a mush. The separation of the two-phase region in these two zones helps to avoid ambiguity when different mechanisms of liquid-solid interactions are attributed to the different stages of solidification.

Despite a good amount of literature available on DC cast Al alloys, the effect of GR with respect to macrosegregation remains unclear, and relatively few articles are available on this subject.[4–12] These studies greatly vary in assessing the effect of GR on macrosegregation. Negative centerline segregation of Cu and Mg with a corresponding positive segregation of Ti was observed in grain-refined sheet ingots of an Al-Cu-Mg alloy.[4] Work by Gariepy and Caron[5] on commercial Al alloys showed that GR practices influenced the level of centerline negative segregation, which, for example, was more than doubled by the addition of grain refiners to a 5182 alloy. Glenn *et al*.[8] also observed greater centerline depletion of Mg in a grain-refined AA 5182 alloy, as did the studies by Lesoult *et al*. and Joly *et al*.[7,9] on Al-Mg alloy sheet ingots. However, the opposite trend was observed by Finn *et al*.,[6] who reported that GR produced positive centerline segregation on a large Al-Cu round billet. On the

other hand, recent work on various commercial alloys at the authors' laboratory showed that GR did not affect the macrosegregation.[10–12]

The detrimental effect of GR on macrosegregation is ascribed to the nucleation of a larger number of free-floating dendrites at the solidification front (in comparison to the non-grain- refined (NGR) sample) and consequent sweeping of those to the bottom of the sump.[5] This is based on the mainstream concept applied to NGR billets/ingots that the so-called "floating" grains, being solute-lean, contribute to the negative centerline segregation. In the billet structure these floating grains appear as dendritic grains with coarser (thicker) dendrite branches (larger dendrite arm spacing, or DAS). In this article, such grains will be called coarse-DAS grains as contrasted to the grains with the finer internal structure, *i.e.*, fine-DAS grains. It is important to note that the grain sizes for both types of dendrites are close, so the terms "coarse" and "fine" grains are somewhat ambiguous. Duplex microstructures (mixture of coarse- and fine-DAS grains) in GR samples are also observed though seldom reported.[4,6,11,12] Doubts have been expressed as to what extent the coarse-DAS grains affect the macrosegregation,[13] and studies exist where larger negative centerline segregation is observed even in the absence of coarse-DAS dendrites in a GR ingot (as compared to the NGR ingot with duplex microstructures but lesser segregation).[7] To add to the controversy, Glenn *et al.*[8] invoked the formation and distribution of "showering crystals." They argued that in all cases, small showering crystals were responsible for the negative centerline segregation. In this case, the formation of large showering crystals, whose average solute content is higher than that of the small showering crystals, can actually lower the magnitude of negative segregation in the central zone of an NGR billet. This line of argument is similar to the one proposed by Chu and Jacoby,[14] who suggested that the fine-DAS dendrites are solute-poor and contribute to the negative centerline segregation.

The positive segregation, which was observed in a grain-refined 530-mm billet of an Al-4.5 pct Cu alloy,[6] despite the observation of duplex microstructures (*i.e.*, with possible solute-lean grains) was attributed to the high permeability in the two-phase region that allowed advection of solute-rich liquid (buoyancy-driven flow) toward the centerline. In the case of NGR billets (columnar structure) that had a less permeable mush with reduced advection, the shrinkage-driven flow produced negative centerline segregation.

Our earlier articles on various commercial Al alloys show that the addition of an Al-Ti-B grain refiner does not affect the macrosegregation in 200-mm billets cast at 80 to 120 mm/min.[10–12] Considering the nature of microstructures and the amount of coarse-DAS grains, it is inferred that mushy-zone permeability might be high enough so as to compensate by liquid transport the depletion of alloying elements caused by solute-lean grains. A single study has shown that increasing amounts of grain refiner increases the magnitude of segregation.[5] The tendency for segregation is also dependent on the type of grain refiner[5,8] (*e.g.*, Al-Ti *vs* Al-Ti-B), which means that structural refinement may directly affect the macrosegregation.

The presumption as to whether the coarse-DAS dendrites are solute-depleted is another contentious issue to be looked into. Next, the question arises as to the role of coarse-DAS grains in case of GR billets. Despite the availability of already mentioned literature on DC cast Al alloys, there has been little systematic work concerning the effect of GR on macrosegregation with reference to the experimental data and associated structural evolution. With this objective in mind, an experimental program involving several DC casting experiments has been launched to examine the effect of GR on microstructural evolution and macrosegregation of various commercial wrought Al alloys. This article reports the work carried out on an AA2024 (Al-Cu-Mg) alloy.

II. EXPERIMENTAL METHODS

Commercial-scale DC casting experiments were conducted in a pilot DC casting installation at the Delft University of Technology. The equipment consists of an electrical resistance tilting furnace (which can hold up to 200 kg of molten metal), a fixed trough with a launder (delivery system), and a 196-mm hot top mold fitted into a water box. The hot top has a total height of 170 mm, which is inserted into a water-cooled aluminum-alloy mold with an efficient mold height of 20 mm. Prior to the experiment, the launder was preheated to about 500 °C. The melt from the furnace passes through the launder and enters the hot top from one side; hence, this is a level-pour system. The melt level in the hot top was 140 mm above the bottom of the hot top. This level was controlled during casting by a laser melt-level controller with the feedback to the tilting furnace. The melt level was maintained within ± 10 mm of the set point. A detailed description of this unit can be found elsewhere.[15,16]

Experiments were carried out with and without GR using an AA2024 alloy, with the composition as given in Table I. Considering the strong influence of casting

Table I. Nominal Composition of AA2024 (Weight Percent) and Alloy Used in This Work

Alloy	Cu	Mg	Fe	Si	Mn	Cr	Ti	Al
Standard	3.8 to 4.9	1.2 to 1.8	0.50 max	0.50Si max	0.3 to 0.9	0.10 max	0.15 max	bal
Alloy used	3.5	1.41	0.144	0.082	0.37	0.006	$<0.0013^{*}$	bal

*Below the detection limit of the spark spectrum analyzer.

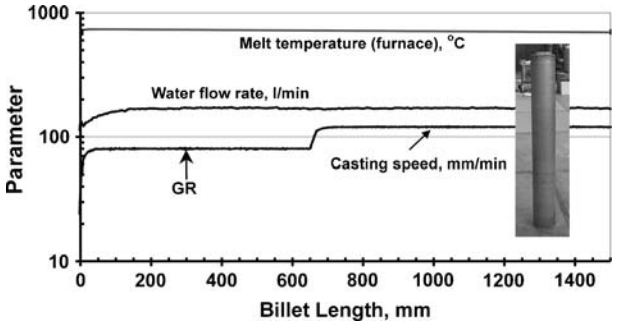

Fig. 1—Process chart for the DC casting experiment of AA 2024; insert: typical DC cast billet, 1500-mm length. Grain refiner was introduced in experiment 1 at the location "GR."

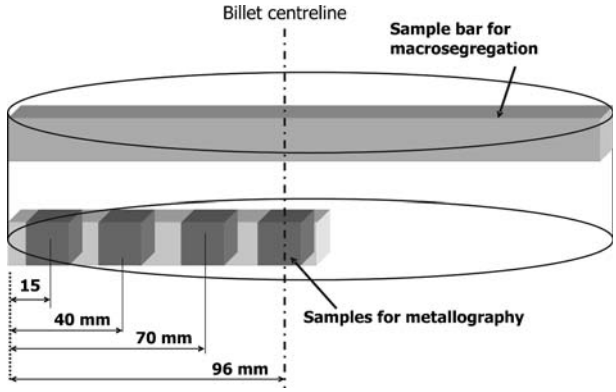

Fig. 2—Scheme of sampling in the billet exhibiting the specimen (upper) used for macrosegregation measurements and (lower) for microstructural characterization.

speed on the macrosegregation, in our casting trials, two casting speeds (80 and 120 mm/min) were used while maintaining constant water flow rate (170 l/min) and melt temperature in the furnace (720 °C). The process chart for a typical DC casting experiment is shown in Figure 1. The temperature drop (typically of about 40 °C) during the melt transport in the launder is measured by placing a thermocouple in the launder close to the melt entry to the hot top. Grain refiner was added in the form of commercial Al-3 pct Ti-1 pct B master alloy rod in the furnace and/or manually in the launder. In the first experiment, the grain refiner was introduced in the launder after some length had been cast at a speed of 80 mm/min, and further when the casting speed was increased to 120 mm/min as shown in Figure 1. The second experiment was conducted with a similar process chart with a grain-refined melt prepared in the furnace. To accomplish this, a known quantity of grain refiner (2 kg/tonne) was added to the liquid metal in the furnace just prior to commencing the DC casting. In this experiment, further additions of grain refiner were made manually through the launder. In this way, samples with various amounts of grain refiner were obtained, and Table II lists the sample designations along with the level of Ti measured in all the cases.

All microstructural observations and macrosegregation measurements were made along the billet diameter in the direction perpendicular to the melt inlet into the hot top (if not stated otherwise). After casting due to the thermal contraction, the billet has a diameter of 192 mm. The billets were longitudinally sectioned in the center plane, and rectangular bars approximately 20-mm wide and 20-mm high were cut in the horizontal cross section of the billet (Figure 2). The samples were cut from the sections of the billet cast at least 200 mm after the startup or the change of the casting speed to ensure steady-state conditions. Composition measurements were carried out by a spark spectrum analyzer SPECTROMAX* on all four sides of each bar at regular intervals of approximately 10 mm, and the average values of four measurements are reported. In addition, the chemical composition at the billet surface was analyzed. The absolute statistical error in these measurements is 0.05 wt pct for Cu and 0.02 wt pct for Mg. For microstructural observations, smaller samples were cut at different locations along the billet radius, as shown in Figure 2. Observations are initiated at a distance of 15 mm from the billet surface so as to eliminate the surface effects, which can induce structural heterogeneities (*e.g.*, a minimum grain size or dendrite arm spacing (DAS)) on account of direct water impingement and coarser structures due to air gap formation.[15] This first sample is always referred to as "subsurface" for subsequent discussion in the rest of the article. Grain size and morphology were studied under cross-polarized light after anodizing the samples in a 3 pct HBF_4 water solution. Other structure features such as DAS and floating grains were revealed after etching the samples with 0.5 pct HF water solution. Grain size and DAS were measured on

*SPECTROMAX is a trademark of Spectro Analytical Instruments GmbH & Co., Kleve, Germany.

Table II. Sample Designation and Ti Concentration

Sample	Casting Speed, mm/min	Ti, Pct	Method of Addition	Code
Non-grain-refined	80	< 0.0013*	—	NGR
Grain-refined	80	0.006	furnace	GR-FC-8
Grain-refined	120	0.008	furnace	GR-FC-12
Grain-refined	120	0.024	launder	GR-L-12
Grain-refined	120	0.04	furnace + launder	GR-FCL-12

*Below the detection limit of the spark spectrum analyzer.

photographs using the random line intercept technique. In all cases, statistical analysis of the results was performed.

Line scan measurements with electron probe microanalysis (EPMA) were carried out on selected samples to assess the variation of local composition across the dendritic microstructures with different DAS.

III. RESULTS

A. *Macrosegregation*

Composition profiles of the major alloying elements (Cu and Mg) plotted across the whole diameter (192 mm after cooling to room temperature) indicate negative segregation in the center and minor positive segregation at the midradius. Further, strong segregation zones are noticed close to the surface.

The effect of grain refinement on the macrosegregation profiles for the casting speed of 80 mm/min is shown in Figure 3. At this casting speed, it can be seen that GR does not seem to have a significant influence on the composition profiles, although a slight shift toward the negative segregation in the center and less subsurface segregation could be noticed upon GR. On the other hand, at a higher casting speed of 120 mm/min, deeper segregation levels are revealed, particularly in the central portion of the billet (Figure 4), irrespective of the grain refiner amount and the method of addition. The increase in the amount of grain refiner seems to change somewhat the macrosegregation profile, but note that the differences in absolute concentrations are very small, being 0.04 pct Cu and 0.02 pct Mg. The segregation pattern varied depending on the element under consideration, with Cu exhibiting higher variation as compared to Mg. This point is further illustrated in Figure 5, where Fe shows a deeper segregation profile compared to Cu and Mg (Figure 4(a)), while Mn exhibits almost no macrosegregation. Further, Ti enrichment is noted in the central portion of the grain-refined billet (Figure 5). In all the cases, strong positive (negative in case of Ti) segregation of alloying elements is observed on the billet surface. From the above trends, it is apparent that the casting speed has more influence on macrosegregation as compared to grain refining.

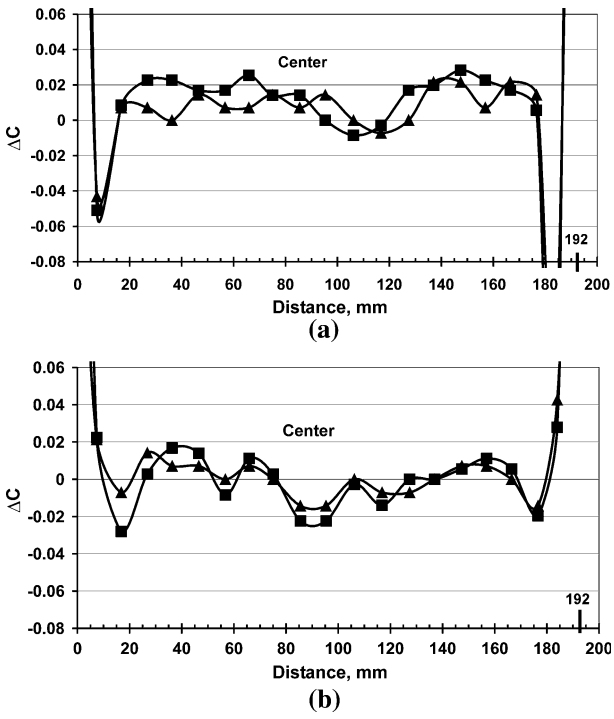

Fig. 3—Macrosegregation profiles at a casting speed of 80 mm/min: Cu (■) and Mg (▲) for billets of (*a*) NGR, (*b*) GR-F-8 (0.006 pct Ti), $\Delta C = (C_i - C_{ave})/C_{ave}$ (relative deviation of concentration from the average), where C_i is the concentration at the radial position and C_{ave} is the average concentration.

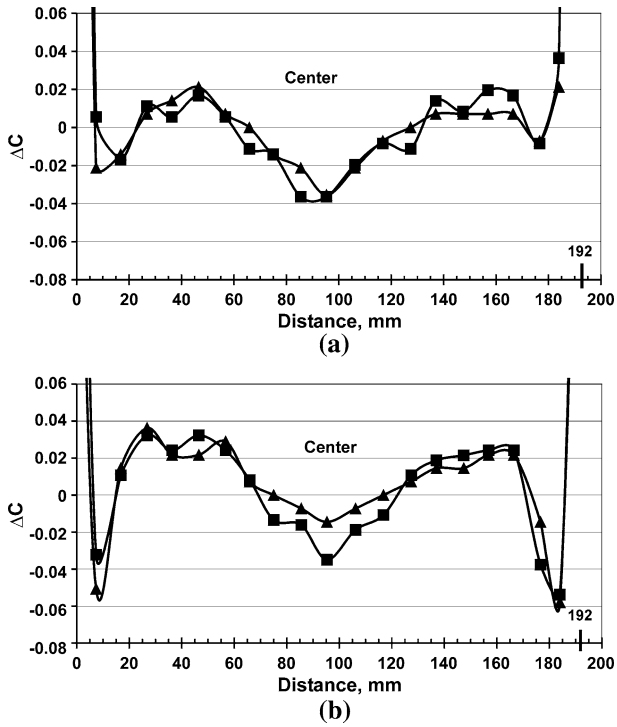

Fig. 4—Macrosegregation profiles at a casting speed of 120 mm/min: Cu (■) and Mg (▲) for billets of (*a*) GR-F-12 (0.008 pct Ti) and (*b*) GR-FL-12 (0.04 pct Ti). ΔC is defined in Fig. 3.

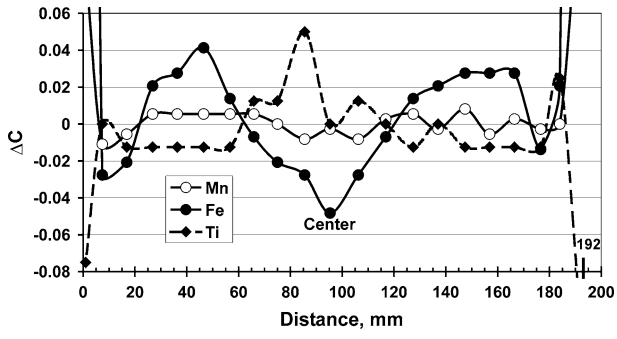

Fig. 5—Macrosegregation profiles of Fe, Mn, and Ti for the grain-refined (GR-F-12, 0.008 pct Ti) billet at a casting speed of 120 mm/min. ΔC is defined in Fig. 3. The data for Ti are divided by 10.

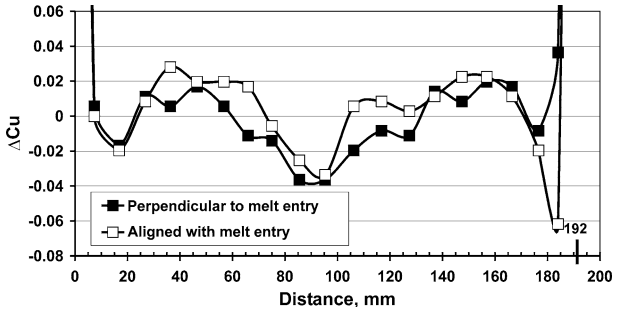

Fig. 6—Macrosegregation profiles of Cu at a casting speed of 120 mm/min (GR-FC-12) taken along two billet diameters, aligned with the melt inlet and perpendicular to the melt inlet.

The level-pour method of melt delivery in the hot top can cause asymmetrical flow pattern in the sump of the billet with consequences for the macrosegregation pattern. Therefore, in our research we always studied the diametral section of the billet that was perpendicular to the melt inlet, and the results should be comparable and not biased by the position of the examined section. Nevertheless, we checked for the importance of the chosen section with respect to the macrosegregation results. Macrosegregation profiles were measured in two perpendicular cross sections of the billet in the directions that were parallel and perpendicular to the melt inlet. The results shown in Figure 6 demonstrate that the nature and variation of the segregation profiles are almost the same.

B. *Microstructure*

1. *Grain size*

Equiaxed microstructures across the billet cross section are observed in all the cases, including the NGR billet. Grain refinement is obvious with Al-3Ti-1B additions as low as 0.006 wt pct Ti. On average, at midradius, the decrease in grain size is from 250 to 55 μm. The radial distribution of grain size in different conditions (Figure 7(a)) shows that the grain size coarsens from the periphery to the center of the billet. For the NGR billet, it changes from 200 μm close to the surface to 275 μm in the center. Grain-refined samples exhibited a variation from around 42 to 80 μm. The grain-refined billet with 0.024 wt pct Ti (GR-L-12 sample) shows a finer grain size than the grain-refined billet of 0.008 wt pct (GR-FC-12). However, there is no additional refinement when the percentage of Ti is further increased to 0.04 wt pct (GR-FCL-12, Figure 7(b)). The average refined grain size is about 50 μm (Figure 7(b)) under different casting speeds and amounts of Al-3Ti-1B master alloy. It can be seen that casting speed has only a minor effect on the grain refinement in GR billets (compare GR-FC-8 and GR-FC-12 in Figure 7(a)).

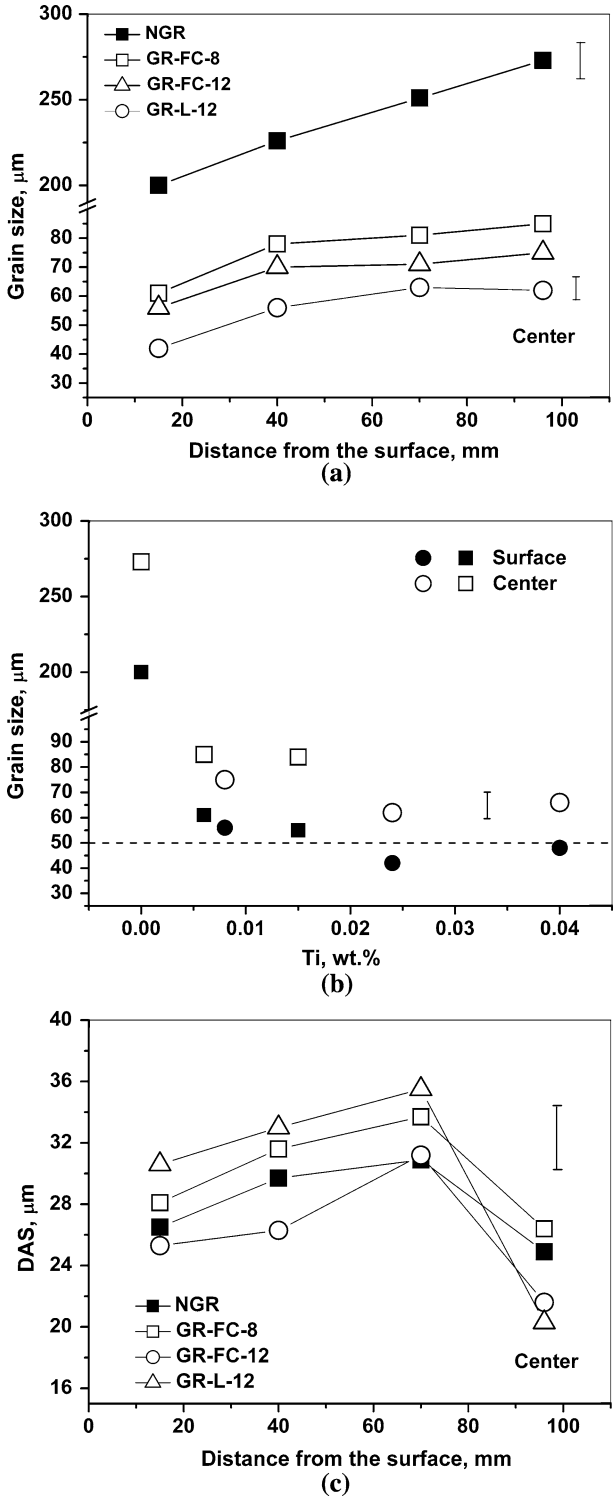

Fig. 7—(*a*) Radial distribution of grain size, (*b*) the effect of Ti content on the grain size, and (*c*) radial distribution of DAS.

2. *DAS and coarse-DAS grains*

The radial variation of DAS (Figure 7(c)) shows an increase toward the center but exhibits a sudden decrease in the center. It should be mentioned that the presence of coarse-DAS grains in the center were not taken into account, and measurements were confined only to the grains with finer DAS.

A characteristic feature of the microstructure in all the samples is the occurrence of duplex structures in the central portion of the billet. Irrespective of grain

refinement, the etched microstructures reveal grains with a coarser DAS coexisting with regions of finer-DAS dendrites in the central portion of the billet (Figures 8 and 9). The coarse-DAS dendrites are seen clustered together in the grain-refined samples (Figures 8(h) and 9(b) and (d)). Histograms of DAS measurements show a broader variation in the center as compared to the subsurface structure (Figures 8(e) and (j) *vs* Figures 8(d) and (i)). At a higher casting speed, this trend can be seen in the all grain-refined samples despite the great variation in Ti content (Figure 9). The volume fraction and the DAS data for coarse- and fine-DAS grains are given in Table III. The coarse DAS of apparently floating grains is around 2.5 to 3 times that of the finer DAS within the duplex structures.

Not only the presence of coarse-DAS grains, but also their distribution across billet cross section, is of interest. Observations on all the samples indicated that duplex structure, hence the coarse-DAS grains, is present essentially in the central portion of the billet, around 20 mm from the central axis (Figure 8). The morphology of grain-refined samples varies with the location and the amount of grain refiner (Figure 9). Closer to the surface, little branched grains appear at a higher Ti contents (≥ 0.024 pct Ti in the present case). From this point and toward the centerline, a cellular-dendritic structure is gradually developed. In view of their size, the grains show rudimentary dendritic arms but not regular dendritic network. Closer to the center, dendritic microstructure persists in the fine-DAS grains of the duplex microstructures. Within the coarse-DAS grains, the tendency is toward less dendritic structures (*i.e.*, without discernible dendrite arms) at higher Ti levels. In the samples with a lower Ti content (0.006–0.008 pct Ti), at both given casting speeds, the coarse-DAS grains are always dendritic (Figures 8(h) and 9(b)).

3. *Microsegregation Measurements*

To ascertain the importance of coarse-DAS grains with respect to centerline segregation, local composition measurements were carried out by EPMA on several coarse and fine dendrite branches in both NGR and GR-FC-8 samples. Examples of such line scan are shown in Figure 10. Care was taken so that the analysis was performed, wherever possible, along the central part of the dendrite branches. The results were very consistent and reproducible for different measured dendrite branches. In both conditions, it can be seen that coarse dendrite arms have a minimum concentration plateau in the central part of the dendrite arm (Figures 10(a) and (c)). On the other hand, finer dendrite arms do not exhibit such a plateau, and concentration varies continuously till the center of the arm (Figures 10(b) and (d)). The minimum elemental concentrations for coarse and fine dendrite arms are given in Table IV. Despite some scatter in the measurements for the fine-DAS grains, it is observed that these minimum concentrations are always higher than those in the coarse-DAS grains for both NGR and grain-refined samples. According to the only article where such measurements have been performed,[4] this means that coarser-DAS grains are more solute depleted as compared to the "regular," finer-DAS grains. Further, it can be mentioned that grain refinement does not seem to make much difference for the minimum concentration. Note that the nominal composition of this alloy is 3.5 wt pct Cu and 1.4 wt pct Mg (Table I).

IV. DISCUSSION

The macrosegregation profiles and microstructures shown in this article were obtained in identical sections of the billets. In addition, the macrosegregation profiles taken in perpendicular sections of the billet are very close to each other (Figure 6). Similar comparison for other alloy compositions and casting conditions have been reported earlier.[15] We believe that the macrosegregation profiles shown elsewhere in this article are representative and not biased by the melt delivery.

The addition of even small amounts of Al-3Ti-1B master alloy leads to efficient refinement of grain size, which can be attributed to the high value of growth restriction factor (GRF) for this alloy.[17] The increase in grain size toward the center, which is consistent with the earlier observations,[8,15,18,19] is due to the decrease in heat extraction rate from the surface to the center. Titanium enrichment is observed in the center of the grain-refined billets (Figure 5). This factor can, in principle, decrease the grain size. But, in absolute terms, this increase in Ti concentration is not significant and hence might have only a little effect on the final grain size in the center. With respect to the grain refiner amount, the decrease in grain size is not much above 0.008 pct Ti and, more importantly, there is no additional effect of grain refiner above 0.024 pct Ti (Figure 7(b)). Although statistically it appears that a larger number of nucleants can facilitate more nucleation events (and thereby decreasing grain size), it is not the case. This is due to the fact that as the amount of inoculant particles participating in nucleation (at a given undercooling) increases, so does the latent heat release leading to recalescence at a smaller undercooling, thereby lowering the efficiency of the grain refiner.[20] Data from model experiments justify this point.[21]

It was stated that the grain size refinement with increasing concentration of grain refiner is more pronounced as the billet center is approached.[19] Our data do not show such a variation (Figure 8) and this means that GR is not so sensitive to the local solidification conditions in our experimental range and makes the alloy less sensitive to the cooling rate, except at the subsurface where greater refinement is observed. This is further illustrated in the radial distribution of grain size for the grain-refined billets (Figure 7(a)) where the variation is less pronounced as compared to NGR sample. The increase in casting speed to 120 mm/min marginally decreases the grain size at a constant Ti content contrary to a more pronounced effect in DC cast NGR billets.[15,16]

Dendrite arm spacing, however, is more sensitive to the cooling rate, and thus variation in DAS reflects the local solidification time of a particular grain.[15] As it has been observed in the previous works on DC cast Al

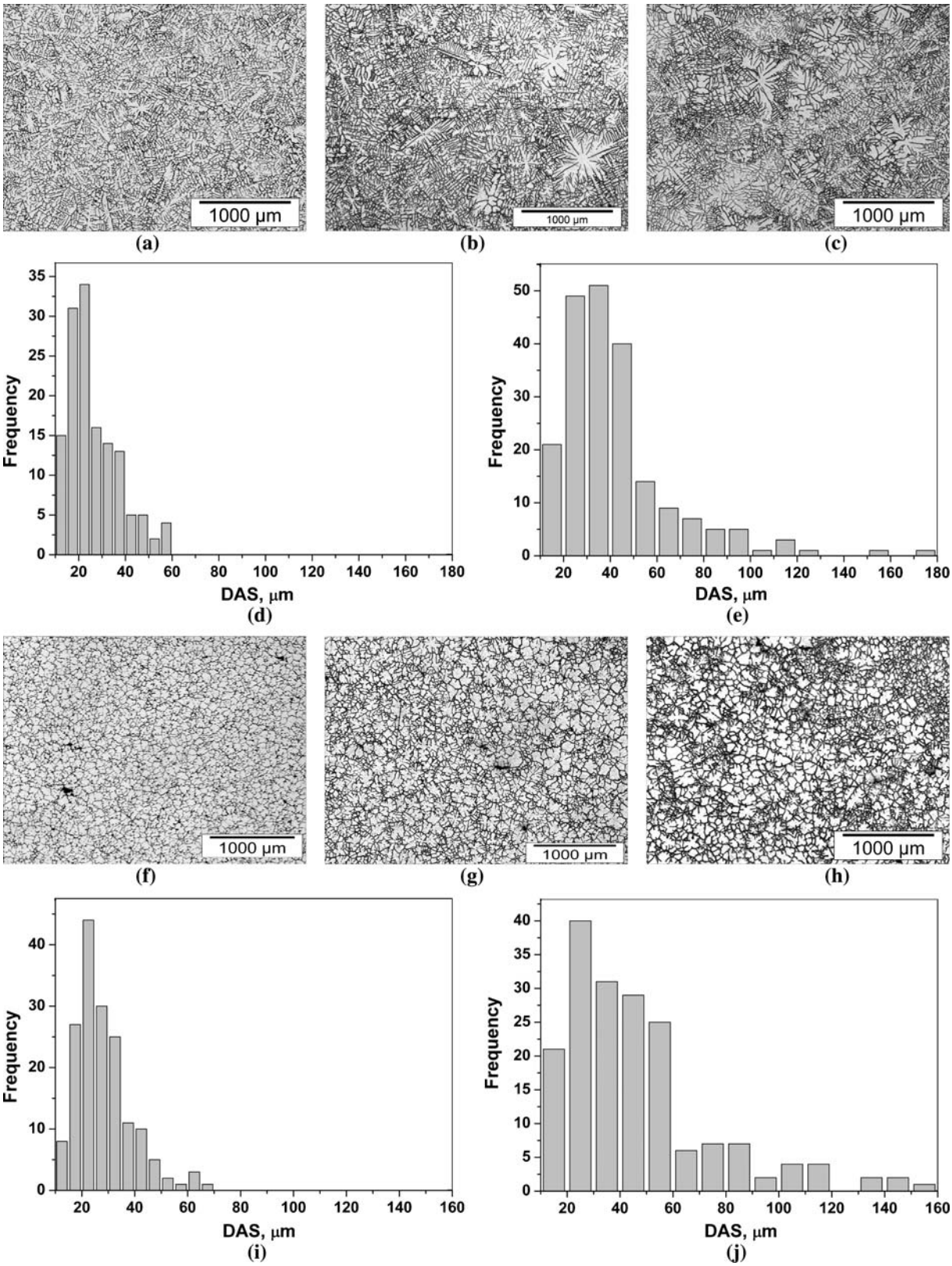

Fig. 8—Appearance and distribution of coarse-DAS dendrites at a casting speed of 80 mm/min along with the histograms of dendrite arm spacing at various locations (distance from the billet periphery): (*a*), (*d*), (*f*), and (*i*) 15 mm; (*b*) and (*g*) 75 mm, where the coarse-DAS grains start to appear; and (*c*), (*e*), (*h*), and (*j*) 96 mm (center). Figs. (a) through (e) refer to NGR billet and (f) through (j) refer to GR billet.

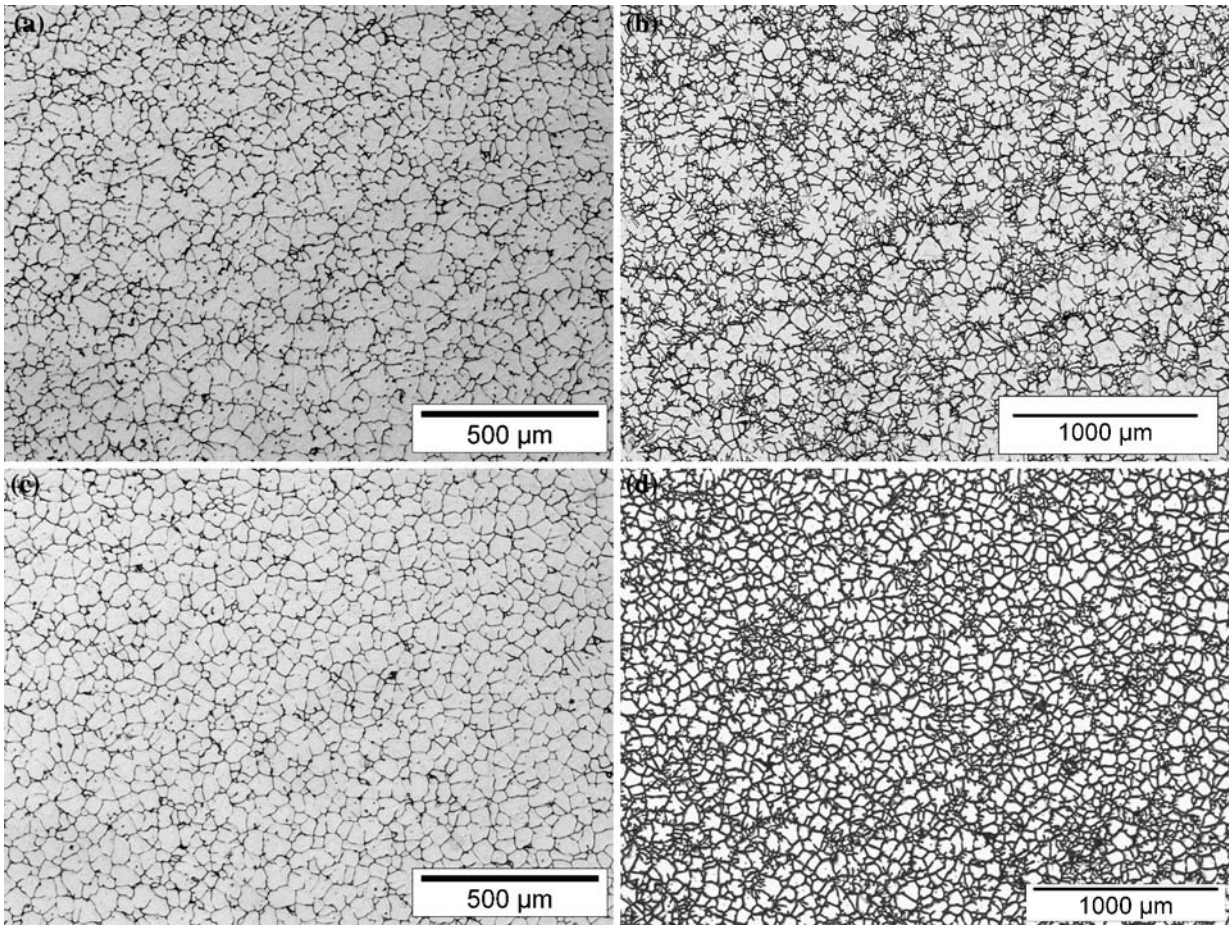

Fig. 9—Microstructures for grain-refined billets cast at 120 mm/min exhibiting duplex microstructures (*b*) and (*d*) in the central portion of the billet as compared to (*a*) and (*c*) at the subsurface. (a) and (b) GR-FC-12 and(c) and (d) GR-FCL-12. The change in grain morphology could be observed at the subsurface with the change in Ti content.

alloys,[6,8,15,16,18,19,22] the DAS increases toward the center in all the samples (Figure 7(c)), due to the continuously lower heat extraction due to water cooling (decreased cooling rate) and widening of the transition region. Though within the error margin, there is a slight refinement of DAS at the higher casting speed. Due to the little branched globular structure, the GR-L-12 sample showed slightly larger DAS.

Another observation is the sudden decrease in DAS at the center, which has been observed in some earlier articles as well.[6,8,19,22] This local refinement of DAS in the center can be explained from the shape of the semisolid region and the way in which the DC cast billet/ingot is solidified. The central part of the billet is formed in the last stage of solidification. This means that the amount of latent heat that is released in a particular horizontal cross section of the billet decreases toward the bottom of the sump, as most of the lower cross section has been already solidified and does not release latent heat anymore. Therefore, the cooling in the central-bottom part of the mushy zone is more efficient than in the slurry zone. Two factors may further enhance the acceleration of cooling in the central part of the billet as compared to an intermediate radial position, as follows: (a) the lower part of the sump (central portion of a billet) is formed, in most cases, in the range of secondary and downstream cooling where the heat transfer is the highest and occurs mostly through the solid phase; and (b) the high solidification-front velocity in the center of the billet may narrow the mushy zone as a result of a higher upward velocity of the solidus isotherm as compared to the liquidus velocity. Note that all this argument concerns only the grains that are formed *in situ*, solidifying from liquidus

Table III. DAS of Different Grains and Volume Fraction of Floating Grains in the Center of the Billet

Sample Code (Table II)	DAS of Coarse-DAS Grains, μm	Approximate Volume Fraction of Coarse-DAS Grains, Pct	DAS of Fine-DAS Grains, μm
NGR	62.7 ± 7.1	35	24.9 ± 1.9
GR-FC-8	65.2 ± 6.2	65	26.4 ± 1.9
GR-FC-12	70.2 ± 6.4	65	21.6 ± 1.4
GR-L-12	58.6 ± 4.5	65	20.4 ± 1.3
GR-FCL-12	49.2 ± 3.2	75	16.8 ± 1.2

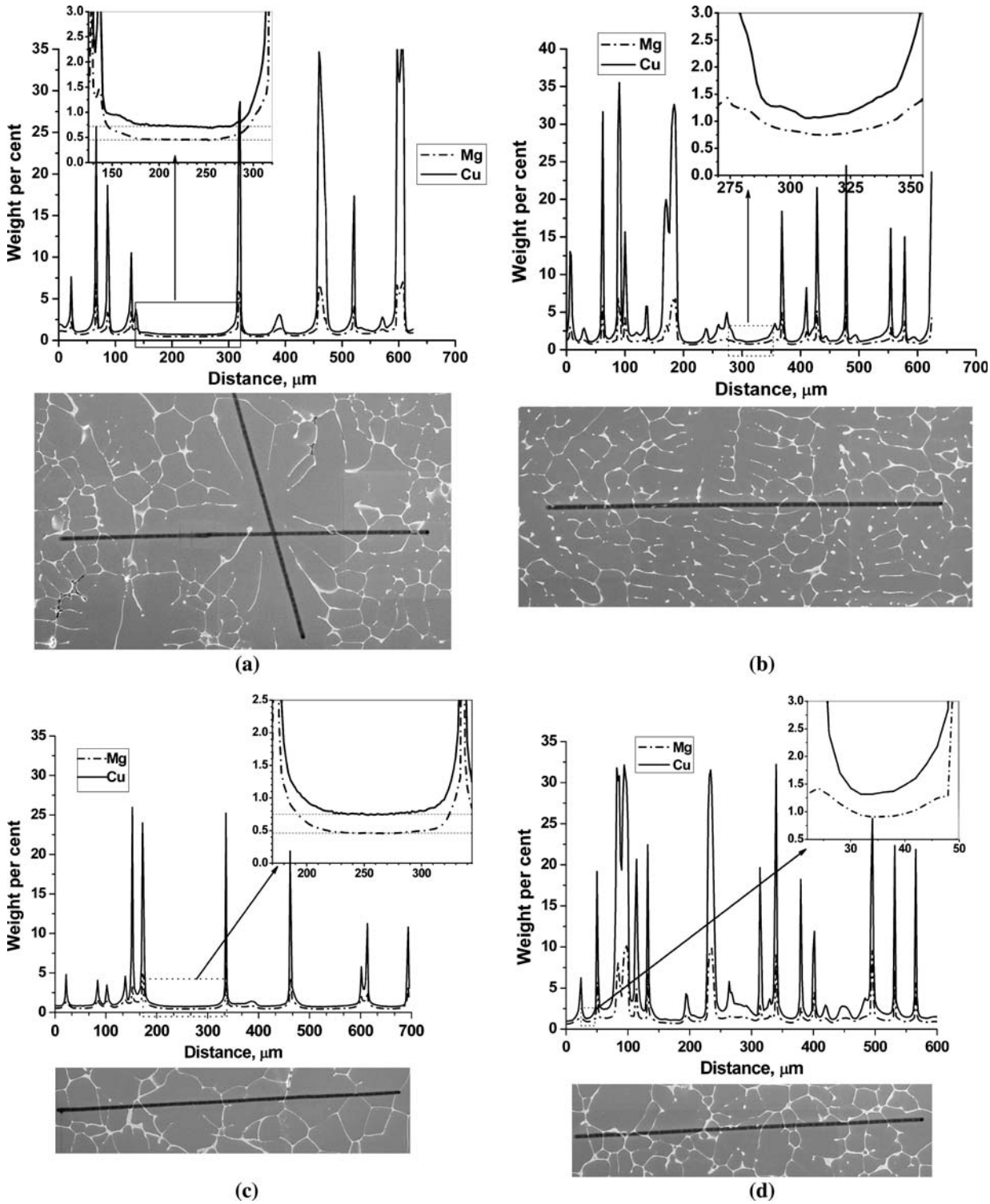

Fig. 10—Microprobe measurements of Cu and Mg concentrations in (*a*) and (*c*) coarse-DAS and (*b*) and (*d*) fine-DAS regions of the (a) and (b) NGR sample and (c) and (d) GR sample. Magnified inserts on plots show the variation of elements between two eutectic boundaries.

to solidus along a downward trajectory, *i.e.*, fine-DAS grains.

The change in grain morphology with the amount of grain refiner and the location (hence, cooling rate) in the grain-refined billets is another interesting observation of this work that has seldom been reported before. The grain structure changes from cellular-dendritic to little branched, globular with increase in both grain refiner amount and cooling rate. As reported elsewhere,[23] higher grain refiner amounts tend to make the grains globular (nondendritic), while higher cooling rates make it more dendritic. Present experimental results are

Table IV. Minimum Concentrations (Weight Percent) in Dendrite Arms Measured during Line Scan

	NGR		GR	
Element	Coarse	Fine	Coarse	Fine
Cu	0.72	1.1	0.75	1.1
Mg	0.45	0.7	0.46	0.7
Fe	0.012	—	0.011	—
Mn	0.30	—	0.30	—
Si	0.026	—	0.028	—

consistent with the literature data that increasing grain refiner amounts facilitate the formation of grains with no visible dendrite arms. However, it is also certain that higher cooling rates lead to less-dendritic grain structures at higher Ti (pattern at the subsurface with changing Ti, Figure 9). One reason could be due to the activation of less potent TiB_2 particles to be involved in solidification at high cooling rates, which may be responsible for the finer grain size. An increase in cooling rate also tries to decrease the DAS, which means it provides an opportunity for the evolving grain to have dendritic branches. Thus it is a balance between how much a grain is allowed to grow and how fine the DAS can be that decides the grain structure. Data indicate that for a grain size lower than 50 μm, grain structure is less dendritic.

Let us now look closer at the phenomenon of coarse-DAS grains. Isothermal dendrites formed early in the solidification process are detached and carried by strong natural convection currents either into the molten metal pool[4] or grow isothermally in the upper part of the transition region before eventually settling to the bottom of the sump. This is supported by numerous experimental observations of a duplex structure both in NGR billets/ingots[14–16,24] and on grain-refined billets,[4,6,12] characterized by a mixture of fine-branched dendrites and coarse-DAS dendrites (Figures 8 and 9). From the micrographs, it is apparent that the structure in grain-refined samples mostly consists of clustered coarse-DAS grains, and it is also quite clear that the coarse- and fine-DAS structures have different origins, as has been discussed earlier for NGR ingots.[15] The larger DAS (Table III) clearly shows that these grains grew much more slowly than the rest of the microstructure.

The fraction of coarse-DAS grains sharply increases with grain refinement. This reflects the delayed coherency of the grain-refined alloy and subsequently a wider slurry zone, which provides more opportunity for small grains to travel within the slurry zone before settling down. (Section I provides definitions of the slurry and mushy zones.)

In general, the relative movement of liquid (rich in solutes with partition coefficient $K < 1$) and solid (solute-lean) phase during solidification in the presence of solute portioning (microsegregation) accounts for the macrosegregation patterns observed in DC casting.[2] The following four important mechanisms are acting together to form the resultant macrosegregation pattern, as follows:

(a) thermo-solutal convection, which transports solute-rich liquid toward the ingot center, resulting in positive centerline segregation (enrichment in alloying elements with partition coefficient $K < 1$);
(b) melt flow in the mushy zone that feeds the solidification shrinkage during solidification, which results in the depletion of alloying elements in the center (negative centerline segregation);
(c) transport of solid grains within the slurry zone due to convective flows and gravity (coarse-DAS grains in duplex structures); and
(d) melt flow in the mushy zone caused by the deformation (*e.g.*, thermal contraction) of the solid network.

The last mechanism is normally associated with the typical surface segregates. The surface region of the DC cast material is often characterized by a strong segregation zone as observed in the present article, which is due to the shrinkage and deformation-driven flows of solute-rich liquid.[4,6] For the centerline segregation, the first three mechanisms are important, and the effect of casting speed and grain refining will be elaborated to explain the observed segregation patterns.

In commercial Al alloys, the degree of segregation depends on the partition coefficients of alloying elements.[5] In the present article, it is observed that the extent of segregation increases with the deviation in K values from unity (Figures 4 and 5). Thus, the propensity toward segregation increases in the following order (with coefficients given in parentheses[5]): Mn (0.90), Mg (0.43), Cu (0.17), Fe (0.03), and Ti (7). Our study indicated that Mn showed negligible segregation tendency irrespective of the casting speed and grain refinement. The phase selection and distribution of coarse constituent particles could be affected with the overall distribution of Fe and Ti.

Casting speed is known to increase the severity of the macrosegregation in DC cast Al alloy billets due to widening of the liquid-solid region, and increase in the steepness of the solidification front, especially in the central portion of the billet.[4,15,25] Experimental measurements in our previous DC casting experiments on AA6061 indeed showed considerable change in the sump depth (~from 25 to 68 mm) as the casting speed increased from 80 to 120 mm/min.[10] On the other hand, grain refinement did not change the sump depth. This means that the increase in the severity of segregation at a higher casting speed (compare Figures 3(b) and 4(a) for the similar Ti content) can be directly related to the expanding distance between the liquidus and the coherency isotherm (the slurry portion of the two-phase region[3]) and the increasing chance of transport of the solute-depleted solid phase toward the center. At the same time, the increased steepness of the solidification front will promote the shrinkage-driven flow of the solute-rich liquid toward the periphery of the billet, resulting in the negative centerline segregation.[25]

The internal structure of equiaxed grains has a profound influence on the coherency and permeability of the mushy zone upon DC casting. In general, grain morphology in commercial grain-refined DC castings is

equiaxed with dendritic substructure.[4,6,8,10,12,19] However, nondendritic grain structures have been reported in DC cast Al alloys upon grain refining.[4,7] Closer to the center, the structure of the coarse-DAS grains is important, and limited reports show that they are either dendritic[6,12] or nondendritic.[4] We found that coarse-DAS grains change their substructure from more dendritic to more globular (less dendritic) with increasing amounts of grain refiner (Figures 9(b) and (d)).

Grain refinement has a dual effect on permeability of the two-phase region. On one hand, it decreases the coherency temperature and effectively widens the slurry region, thereby increasing the permeability of the upper part of the two-phase region. As a result, convective flows have more opportunity to penetrate into the slurry zone and bring solute-rich liquid to the center. On the other hand, the smaller grains decrease the permeability of the coherent mushy zone. This results in less potent shrinkage-induced flow, hence in less negative centerline segregation.

By making the slurry zone wider, the grain refinement also allows far more floating grains. However, these grains are smaller and may be less prone for settling down. But in our experiments, grain refining resulted in a substantial increase in the volume fraction of coarse-DAS floating grains (Table III). Hence, GR can aggravate the negative centerline segregation. The final segregation pattern would be an interplay of different contributions of the discussed mechanisms.

Line scan measurements (Table IV) showed a considerable difference in the elemental concentrations between coarse and fine dendrite arms. The relative immunity to the grain refiner for the local elemental compositions in the coarse-DAS grains (despite the huge difference in their size and morphology, as seen in Figures 8(c) and (h)) may be due to the similar location for growth in the slurry portion of the sump. To the best of our knowledge, only a single study is published[4] where measurements have been carried out on the grain-refined ingot of Al-Cu-Mg. It was shown that the Cu concentration in the central portion of a coarse dendrite arm rapidly falls to 0.7 pct, similar to our data (Table IV). Also, a higher Cu_{min} has been measured within the fine dendrite arms with no plateau, which is in agreement with our results.

Close observation on the measured composition profiles of coarse dendrite arms showed that approximately 50 pct of the dendrite arm section has the minimum (plateau) composition for the NGR case as compared to about 45 pct for the grain-refined case (Figures 10(a) and (c)). Following this and the data in Tables III and IV, a simple calculation can be performed for the grain-refined sample.[4] If we take into account that the fraction of coarse-DAS area (65 area pct of coarse-DAS grains with 45 area pct depleted zone; $0.65 \times 0.45 = 0.29$) has the composition of 0.75 pct Cu and 0.46 pct Mg and assume that the remaining fraction (0.71) at the nominal alloy composition (3.5 pct Cu and 1.4 pct Mg), then the predicted composition at the billet center would be 2.70 pct Cu and 1.13 pct Mg. Assuming that all macrosegregation is caused by the floating grains, this leads to ΔC values of 0.2, which are an order of magnitude larger than the measured values (Figure 3(b)). This offset from the experimental data is, of course, because the other macrosegregation mechanisms also contribute to the total segregation. More refined calculations are necessary, which take into account the distribution of eutectic in both coarse and fine dendrite arms and the morphology of the coarse branches. Further, it would also be interesting to check the local compositions in duplex structures in grain-refined samples of a higher Ti content.

Considering the increased amount of coarse-DAS grains in the present case (approximately 35 pct in NGR samples *vs* around 65 to 70 pct in the grain-refined samples), it appears that increased permeability of the slurry zone and related inflow of the solute-rich liquid into the central part of the billet, along with hindered shrinkage-induced flow in the mush, may partially compensate for the depletion of alloying elements in the center by coarse-DAS grains, thus bridging the gap between NGR and grain-refined billets.

V. CONCLUSIONS

Direct-chill casting experiments with and without GR at different casting speeds were conducted upon casting 192-mm round billets from an AA2024 alloy. Samples with various amounts of grain refiner were studied in detail with respect to the microstructure, existence, and distribution of coarse-DAS (floating) grains and macrosegregation. Significant structural refinement was observed with initial additions of Al-3Ti-1B grain refiner, but higher additions did not induce much further grain refinement. Experimental results showed that grain size and DAS tended to coarsen toward the center. However, a local minimum is observed for DAS in the center on account of local solidification conditions specific to DC casting. In grain-refined billets, grain size did not exhibit great changes with respect to cooling rate and casting speed, although changes in grain substructure (from cellular-dendritic to globular) were noticed. Irrespective of GR and the amount of Ti, duplex structures with coarse- and fine-DAS grains were observed in the central portion of the billet, the fraction of coarse-DAS grains being considerably higher in grain-refined billets.

Macrosegregation patterns showed that the addition of grain refiner did not seem to have any considerable influence, and increased grain refiner amounts did not enhance the segregation tendency. As expected, the severity of segregation increased at a higher casting speed. Elemental segregation tendency is inversely related to their partition coefficient. An increased amount of coarse-DAS (floating) grains together with the increased permeability of the slurry and decreased permeability of the mush seem to compensate for each other and produce the observed trends of macrosegregation under given casting conditions and for the given billet size. The depletion of floating grains is supported by the local composition measurements on the duplex structure, which showed that coarse dendrite branches have a depleted concentration plateau

as compared to the fine dendrite arms, independent of grain refining.

ACKNOWLEDGMENTS

This work is done within the framework of the research program of the Netherlands Institute for Metals Research (http://www.nimr.nl), Project No. MC4.02134. The authors thank J. Pool and M. Bakker for performing the line scan measurements at Corus RD&T (IJmuiden, The Netherlands).

REFERENCES

1. E.F. Emley: *Int. Met. Rev.*, 1976, vol. 206, pp. 75–115.
2. J.F. Grandfield and P.T. McGlade: *Mater. Forum*, 1996, vol. 20, pp. 29–51.
3. L. Arnberg, L. Bäckerud, and G. Chai: *Solidification Characteristics of Aluminum Alloys, Vol. 3: Dendrite Coherency*, American Foundrymen's Society, Des Plaines, IL, 1996, pp. 201–55.
4. H. Yu and D.A. Granger: in *Aluminium Alloys. Their Physical and Mechanical Properties*, E.A. Starke and T.H. Sanders, eds., EMAS, Warley, UK, 1986, pp. 17–29.
5. B. Gariepy and Y. Caron: in *Light Metals 1991*, E.L. Rooy, ed., TMS, Warrendale, PA, 1991, pp. 961–71.
6. T.L. Finn, M.G. Chu, and W.D. Bennon: in *Micro/Macro Scale Phenomena in Solidification*, C. Beckermann, *et al.*, eds., ASME, New York, NY, 1992, pp. 17–26.
7. G. Lesoult, V. Albert, B. Appolaire, H. Combeau, D. Daloz, A. Joly, C. Stomp, G.U. Grün, and P. Jarry: *Sci. Technol. Adv. Mater.*, 2001, vol. 2, pp. 285–91.
8. A.M. Glenn, S.P. Russo, and P.J.K. Paterson: *Metall. Mater. Trans. A*, 2003, vol. 34A, pp. 1513–23.
9. A. Joly, G.U. Grün, D. Daloz, H. Combeau, and G. Lesoult: *Mater. Sci. Forum*, 2000, vols. 329–330, pp. 111–20.
10. R.K. Nadella, D. Eskin, and L. Katgerman: in *Continuous Casting of Non-Ferrous Metals*, H.R. Müller, ed., Wiley-VCH Verlag, Weinheim, Germany, 2005, pp. 277–82.
11. R. Nadella, D. Eskin, and L. Katgerman: *Mater. Sci. Forum*, 2006, vols. 519–521, pp. 1841–46.
12. R. Nadella, D. Eskin, and L. Katgerman: in *Light Metals 2007*, M. Sørlie, ed., TMS, Warrendale, PA, 2007, pp. 727–32.
13. M.C. Flemings: *ISIJ Int.*, 2000, vol. 40, pp. 833–41.
14. M.G. Chu and J.E. Jacoby: in *Light Metals 1990*, C.M. Bickert, ed., TMS, Warrendale, PA, 1990, pp. 925–30.
15. D.G. Eskin, J. Zuidema, Jr., V.I. Savran, and L. Katgerman: *Mater. Sci. Eng.*, 2004, vol. A384, pp. 232–44.
16. D.G. Eskin, V.I. Savran, and L. Katgerman: *Metall. Mater. Trans. A*, 2005, vol. 36A, pp. 1965–76.
17. M.A. Kearns and P.S. Cooper: *Mater. Sci. Technol.*, 1997, vol. 13, pp. 650–54.
18. Suyitno, V.I. Savran, D.G. Eskin, and L. Katgerman: *Metall. Mater. Trans. A*, 2004, vol. 35A, pp. 3551–61.
19. A. Håkonsen, D. Mortensen, S. Benum, and H.E. Vatne: in *Light Metals 1999*, C.E. Eckert, ed., TMS, Warrendale, PA, 1999, pp. 821–27.
20. I. Maxwell and A. Hellawell: *Acta Metall.*, 1975, vol. 23, pp. 229–37.
21. M.G. Chu: in *Light Metals 2002*, W. Schneider, ed., TMS, Warrendale, PA, 2002, pp. 899–907.
22. H. Nagaumi: *Sci. Technol. Adv. Mater.*, 2001, vol. 2, pp. 49–57.
23. M. Easton, J. Grandfield, D. St. John, and B. Rinderer: *Mater. Sci. Forum*, 2006, vols. 519–521, pp. 1675–80.
24. R.C. Dorward and D.J. Beerntsen: in *Light Metals 1990*, C.M. Bickert, ed., TMS, Warrendale, PA, 1990, pp. 919–24.
25. D.G. Eskin, Q. Du, and L. Katgerman: *Scripta Mater.*, 2006, vol. 55, pp. 715–18.